

Electronic Supplementary Material (ESI) for Catalysis Science & Technology.
This journal is © The Royal Society of Chemistry 2016

Electronic Supplementary Information

The effect of CeO₂-ZrO₂ structural differences on the origin and reactivity of carbon formed during methane dry reforming over NiCo/CeO₂-ZrO₂ catalysts studied by transient techniques[†]

Michalis A. Vasiliades^a, Petar Djinović^b, Albin Pintar^b, Janez Kovač^c and Angelos M. Efstathiou^{*a}

^a *Heterogeneous Catalysis Laboratory, Chemistry Department, University of Cyprus, 1678 Nicosia, Cyprus*

^b *Department for Environmental Sciences and Engineering, National Institute of Chemistry, Hajdrihova 19, 1000 Ljubljana, Slovenia*

^c *Department for Surface Engineering and Optoelectronics, Jožef Stefan Institute, Jamova cesta 39, 1000 Ljubljana, Slovenia*

*E-mail address: efstath@ucy.ac.cy

1. Powder X-ray diffraction studies

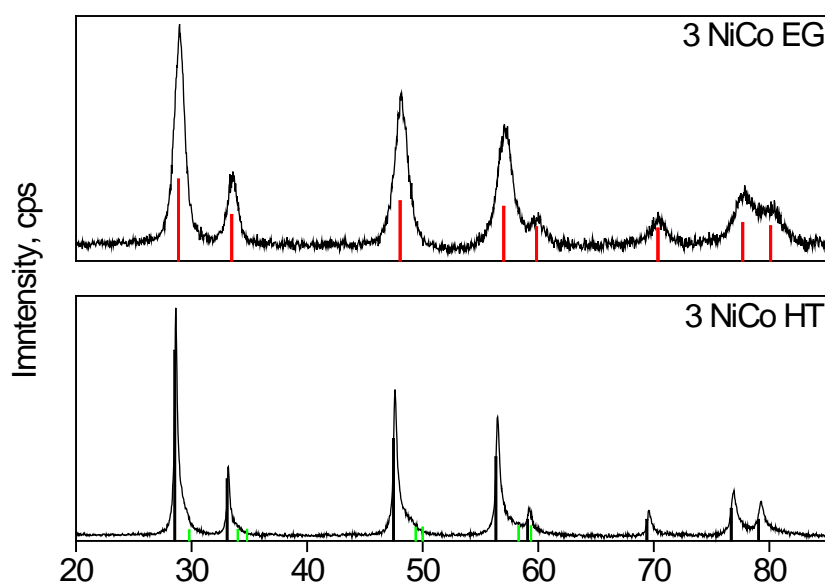


Figure S1: XRD profiles of 3NiCo EG and 3NiCo HT catalyst powder samples recorded according to Experimental Section 2.2. Red bars show the peak positions of $\text{Ce}_{0.75}\text{Zr}_{0.25}\text{O}_{2-6}$ (PDF 28-0271), black bars of CeO_2 (PDF 034-0394) and green bars of ZrO_2 (PDF 01-089-6976).

X-ray spectra were recorded on a PANalytical X'pert PRO diffractometer using $\text{Cu K}\alpha$ radiation ($\lambda = 0.15406 \text{ nm}$). The scanned 2θ range was between 20 and 85° with 0.034° increment and 100 s dwell time at each increment. The instrument induced line broadening and calibration of the 2θ values was performed using a SiO_2 standard. Unit cell size was calculated according to equation: $a = \frac{\lambda}{2} \times \frac{\sqrt{h^2+k^2+l^2}}{\sin \theta}$. In the latter, a parameter represents the crystal unit cell size, λ the X-ray irradiation wavelength, θ the apex position of (111) reflection belonging to CeO_2 phase, with h , k and l being the Miller indices of the (111) crystal plane. The 2θ values, belonging to the reflection from (111) crystalline plane were obtained by fitting the corresponding signal with Pearson VII function in Origin 7.5 software.

2. HR-TEM/EDX studies

Figure S2 shows spatial location of nickel and cobalt in an activated 3NiCo EG catalyst prior to DRM catalytic tests. Nickel and cobalt are found in aggregates which are constituted of both metals in a homogeneous manner (alloy). Based on these results, we can conclude that nickel and cobalt form chemically homogeneous bimetallic particles (NiCo alloy), which are dispersed over the CeZrO_2 solid solution support.

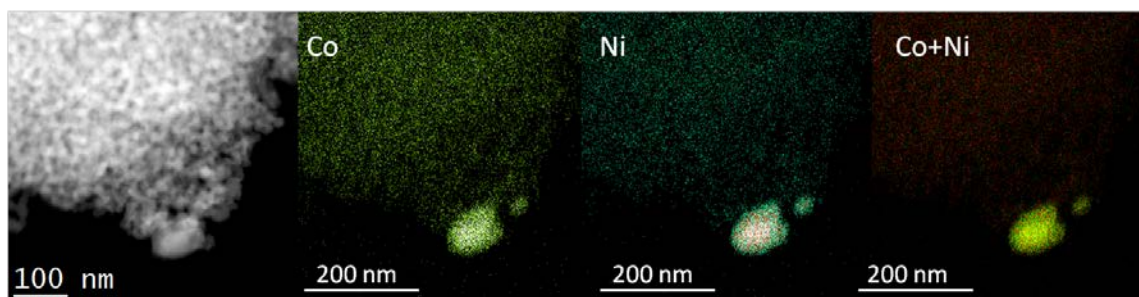


Figure S2: HAADF/STEM micrograph with corresponding EDXS elemental mapping of cobalt, nickel and their overlay on a fresh reduced 3NiCo EG catalyst prior to catalytic tests.

Additional information regarding the structure of bimetallic alloy particles was obtained by performing selected area electron diffraction (SAED) analysis (Fig. S3).

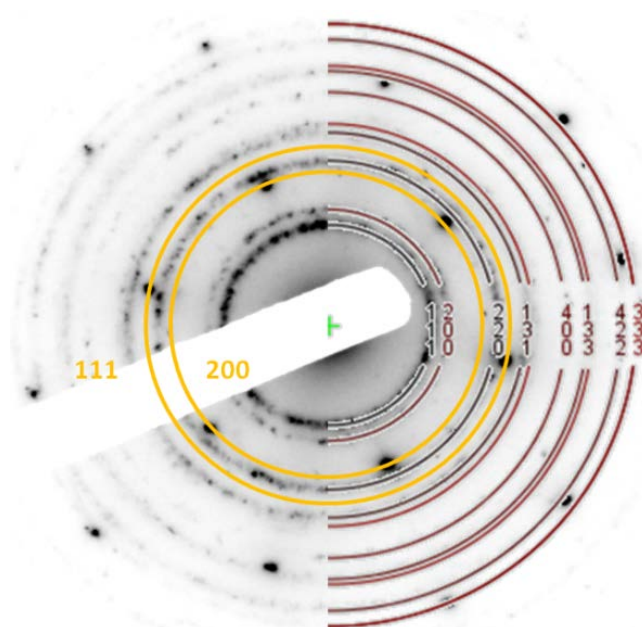


Figure S3: SAED pattern of a fresh reduced 3NiCo EG catalyst prior to catalytic tests.

Two crystalline phases could be identified: a FCC bimetallic alloy comprised of nickel and cobalt. Its most intensive diffraction rings from [200] and [111] crystalline planes are marked with yellow circles.

In addition to diffraction signals originating from NiCo bimetallic phase, additional diffraction rings from support were observed. These could be perfectly simulated by a FCC CeZrO₂ solid solution containing 25 wt.% ZrO₂ (red half circles). No diffraction rings originating from t-ZrO₂ phase could be identified.

HR-TEM analysis identified the presence of bimetallic clusters of varying size (ca. 6 – 15 nm) as shown in the below image (Fig. S4) for the fresh reduced 3NiCo EG catalyst. Similar conclusions were made for the 3NiCo HT catalyst on the basis of similar analyses as for the 3NiCo EG (Figs. S2-S4).

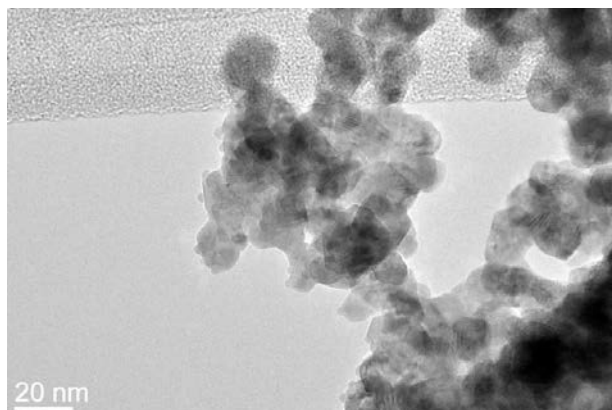


Figure S4: HR-TEM micrograph on a fresh reduced 3NiCo EG catalyst prior to catalytic tests.

TEM-EDX and SEAD analyses confirm that nickel and cobalt are present in the 3NiCo EG catalyst as **alloyed bimetallic nanoparticles** which are dispersed over a support which is comprised of a CeZrO₂ solid solution in a non-uniform manner.

3. Probing the participation of support lattice oxygen in DRM

3.1 ¹⁶O/¹⁸O oxygen isotopic exchange

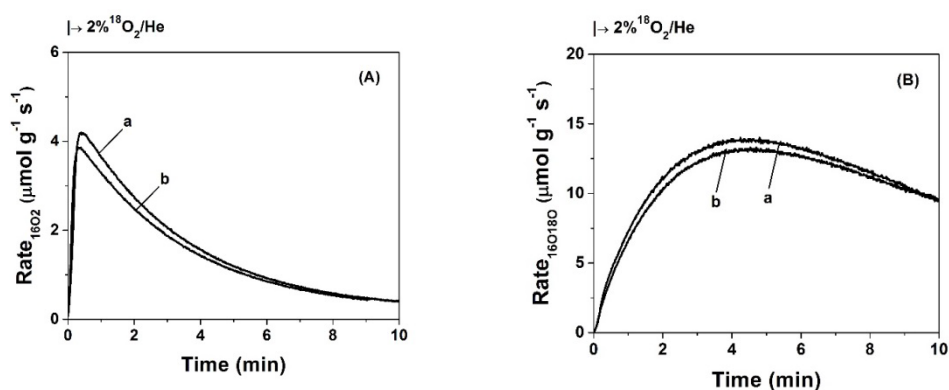


Figure S5: Transient rates ($\mu\text{mol g}^{-1} \text{s}^{-1}$) of $^{16}\text{O}_2$ (A) and $^{16}\text{O}^{18}\text{O}$ (B) formation as a function of time, estimated from the transient isotopic exchange of lattice ^{16}O with ^{18}O experiment according to the gas switch $\text{He} \rightarrow 2\%^{18}\text{O}_2/\text{He}$ performed at 750°C over the 3NiCo EG (a) and 3NiCo HT (b) catalysts. $W_{\text{cat}} = 25 \text{ mg}$.

3.2 20% CO₂/He and x% CO/He gas switch following ¹⁶O/¹⁸O exchange

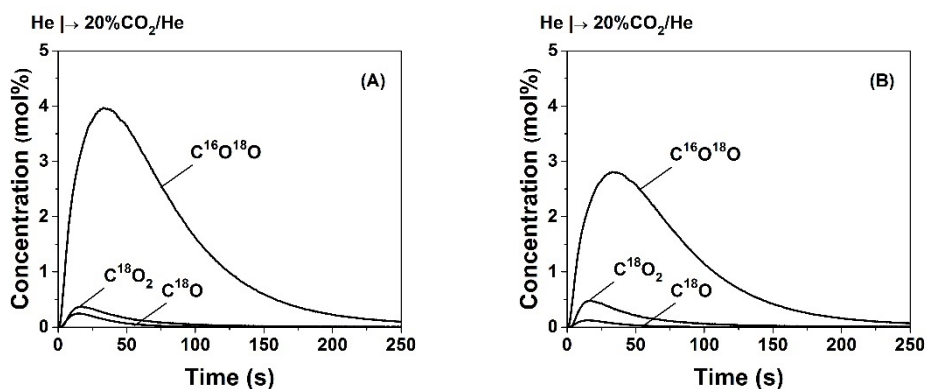


Figure S6: Transient concentration (mol%) response curves of C¹⁸O, C¹⁶O¹⁸O and C¹⁸O₂ obtained at 750 °C after the gas switch He → 20% CO₂/He over 3NiCo EG (A) and 3NiCo HT (B), following catalyst pre-treatment with 2 % ¹⁸O₂/He (10 min) at 750 °C. Gas delivery sequence: He (750 °C) → 2% ¹⁸O₂/He (10 min) → He (5 min) → 20% CO₂/He (t); W_{cat} = 25 mg.

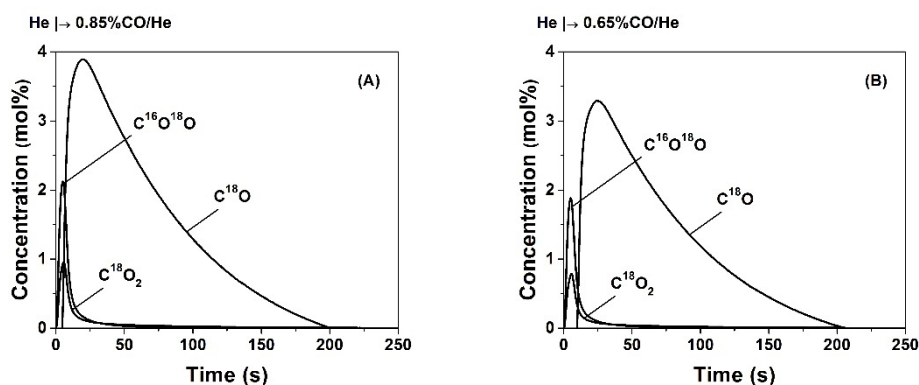


Figure S7: Transient concentration (mol%) response curves of C¹⁸O, C¹⁶O¹⁸O and C¹⁸O₂ obtained at 750 °C after the gas switch x% CO/He over 3NiCo EG (A) and 3NiCo HT (B), following catalyst pre-treatment with 2% ¹⁸O₂/He (10 min) at 750 °C. Gas delivery sequence: He (750 °C) → 2% ¹⁸O₂/He (10 min) → He (5 min) → x % CO/He (t); W_{cat} = 25 mg; x=0.65 and 0.85, respectively, for 3NiCo EG and 3NiCo HT catalysts.

4. Long-term stability in DRM

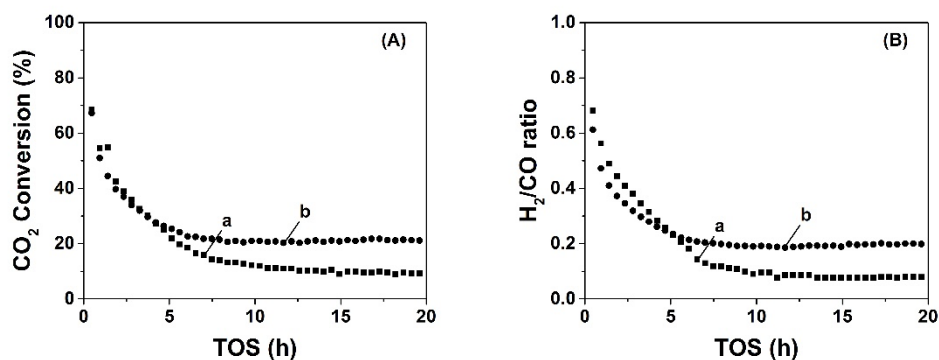


Figure S8: (A) CO₂ conversion and (B) H₂/CO product gas ratio as a function of time on stream (TOS) obtained during DRM at 750 °C for the 3 NiCo EG (a) and 3NiCo HT (b) catalysts. Feed gas composition: 44.2 vol% CH₄, 44.3 vol% CO₂, 11.5 vol% N₂; W_{cat} = 50 mg; F_T = 56.5 NmL min⁻¹.

5. Characterization of “carbon” deposits after 20 h of DRM by HAADF/STEM

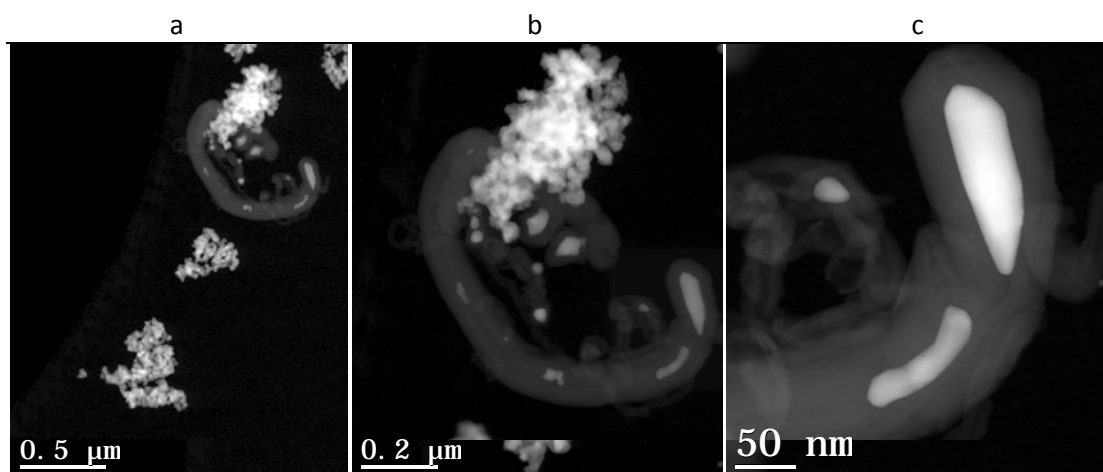


Figure S9: HAADF/STEM micrographs of 3NiCo EG catalyst after 20 h of DRM reaction (44.2% CO₂/44.3% CH₄/11.5% N₂) at 750 °C with progressive magnification.

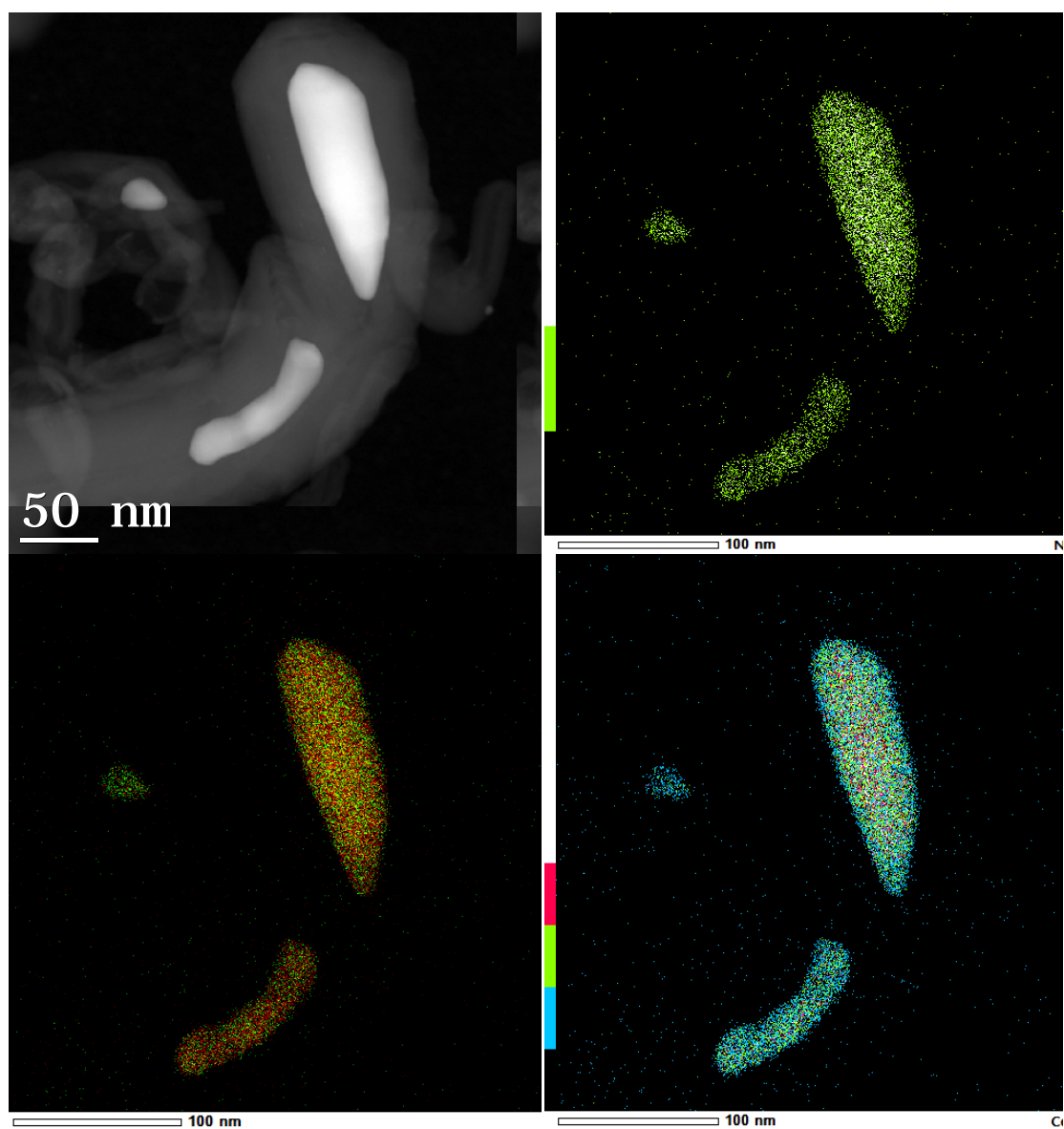


Figure S10: HAADF/STEM micrograph of 3NiCo EG catalyst after DRM reaction at 750°C for 20 h. The image is focused on the NiCo bimetallic particle (top left) with corresponding EDXS elemental mapping: top right nickel, bottom right cobalt, and bottom left nickel and cobalt overlaid.

6. X-ray Photoelectron Spectroscopy Studies

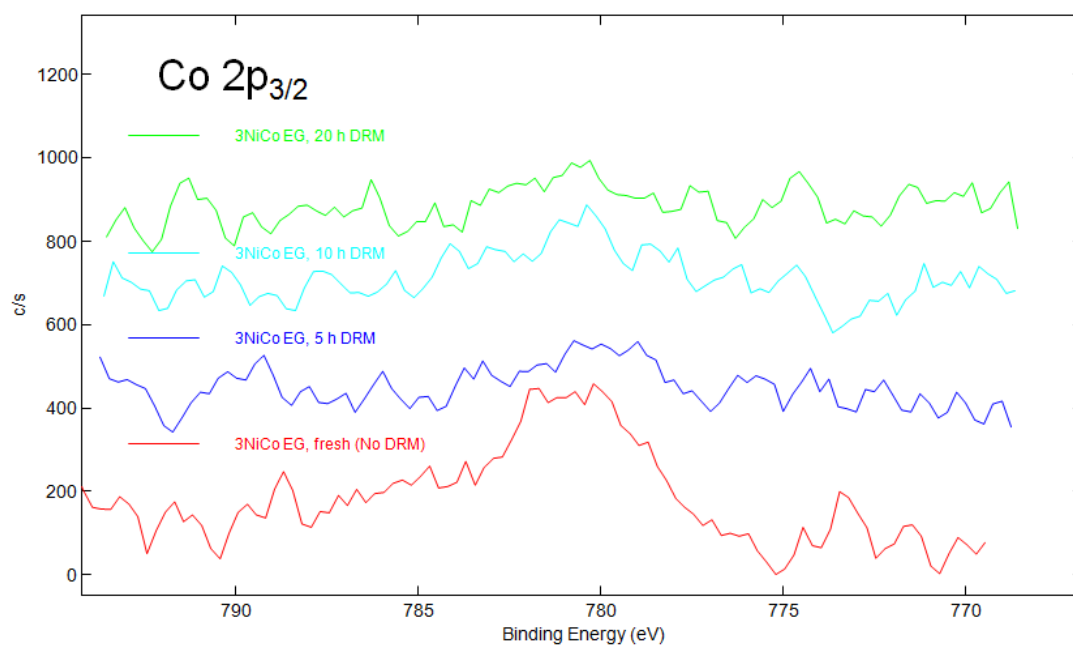


Figure S11: High-energy resolution Co 2p spectra for the 3NiCo EG catalyst recorded at different times on stream (fresh, 5, 10 and 20 h).

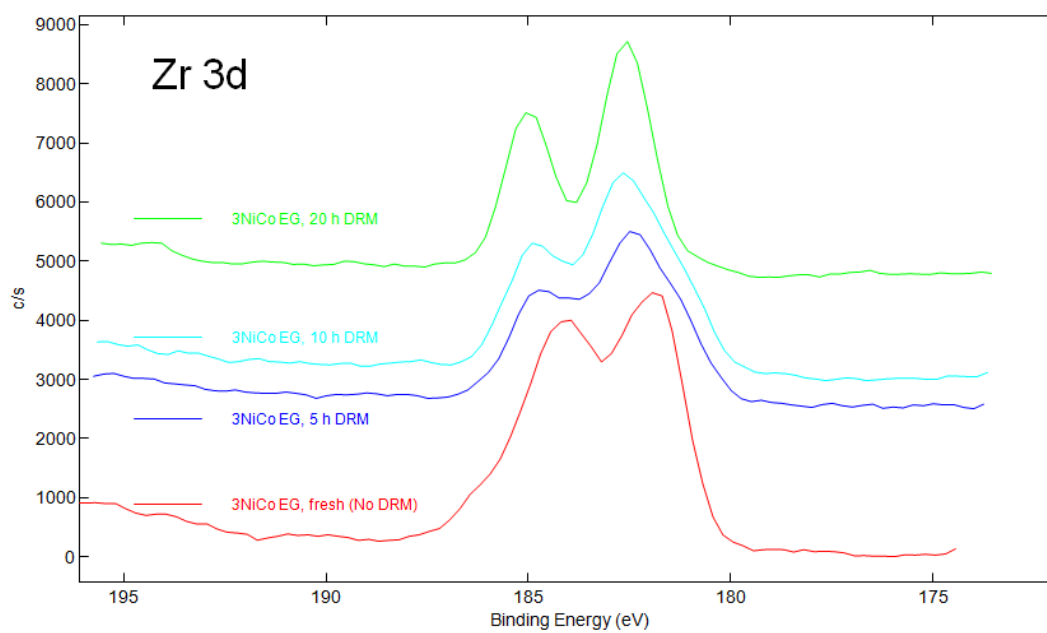


Figure S12: High-energy resolution Zr 3d spectra for the 3NiCo EG catalyst recorded at different times on stream (fresh, 5, 10 and 20 h).

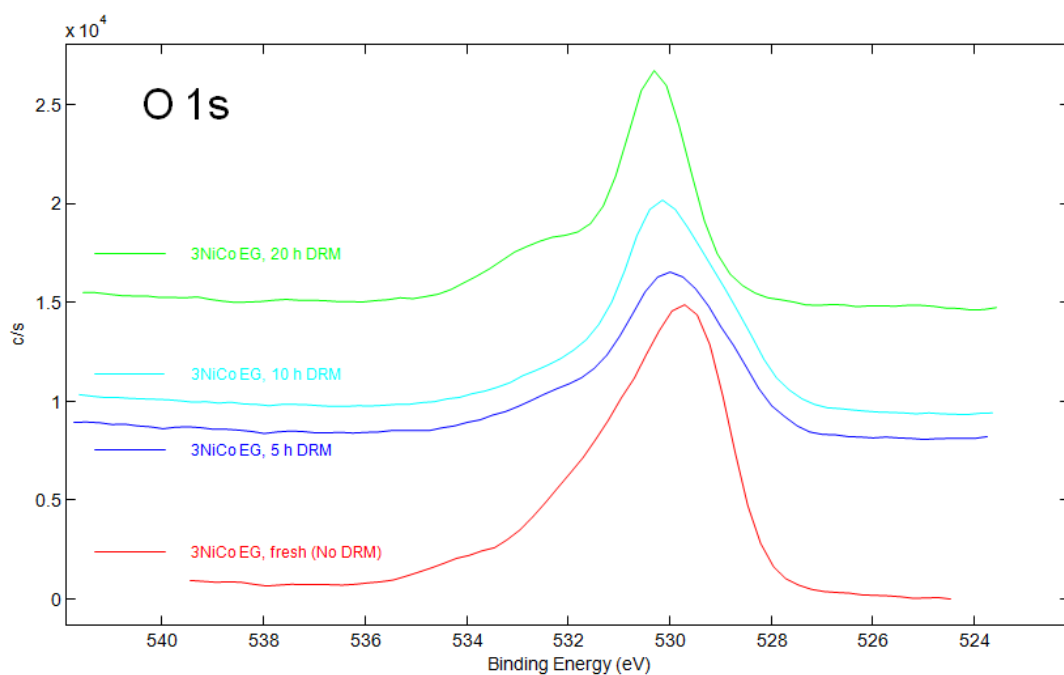


Figure S13: High-energy resolution O 1s spectra for the 3NiCo EG catalyst recorded at different times on stream (fresh, 5, 10 and 20 h).

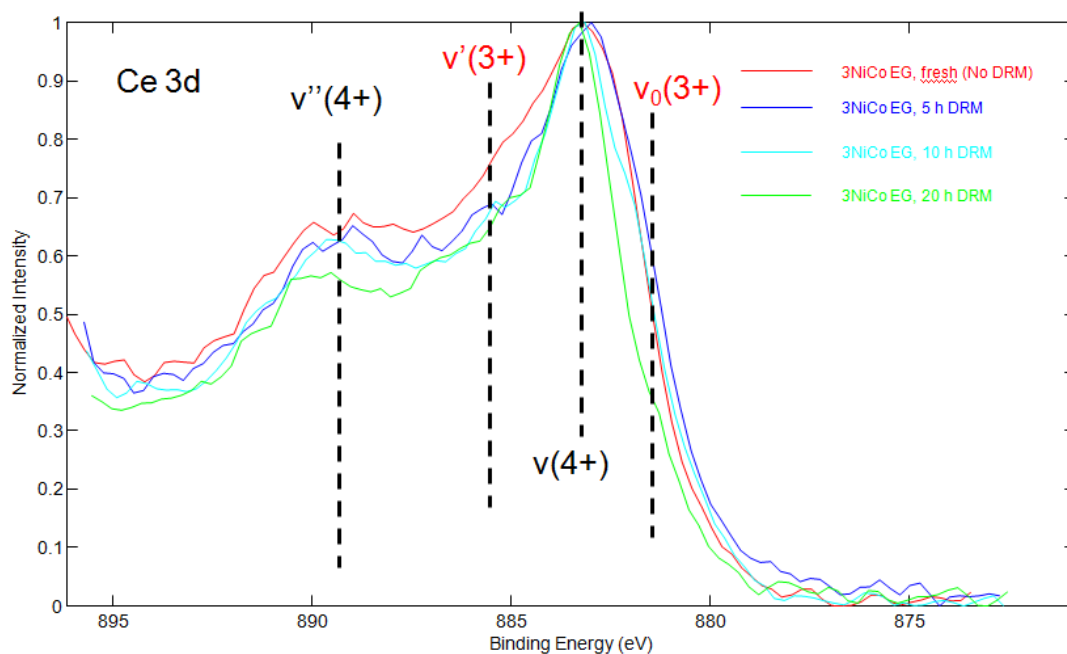


Figure S14: Normalized high-energy resolution Ce 3d spectra for the 3NiCo EG catalyst recorded at different times on stream (fresh, 5, 10 and 20 h).